ACS Biomaterials SCIENCE & ENGINEERING

pubs.acs.org/journal/abseba

Article

Polymer Lung Surfactants Attenuate Direct Lung Injury in Mice

Daniel J. Fesenmeier,[‖] Madathilparambil V. Suresh,[‖] Seyoung Kim, Sungwan Park, Krishnan Raghavendran,* and You-Yeon Won*

Cite This: *ACS Biomater. Sci. Eng.* 2023, 9, 2716–2730

Read Online

ACCESS | Metrics & More | Article Recommendations | Supporting Information

ABSTRACT: If not properly managed, acute lung injuries, either through direct or indirect causes, have the potential to present serious risk for many patients worldwide. One of the mechanisms for the transition from acute lung injury (ALI) to the more serious acute respiratory distress syndrome (ARDS) is the deactivation of the native lung surfactant by injury-induced infiltrates to the alveolar space. Currently, there are no surfactant replacement therapies that are used to treat ALI and subsequent ARDS. In this paper, we present an indepth efficacy study of using a novel polymer lung surfactant (PLS, composed of poly(styrene-*block*-ethylene glycol) (PS-PEG) block copolymer micelles), which has unique properties compared to other tested surfactant replacements, in two different mouse models of lung injury. The results demonstrate that pharyngeal administration of PLS after the instillation of either acid (HCl) or lipopolysaccharide (LPS) can decrease the severity of lung injury as measured by multiple injury markers.

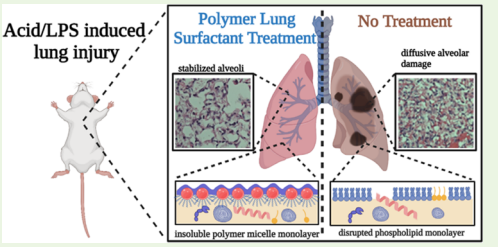

KEYWORDS: *block copolymer micelle, polymer lung surfactant, surfactant replacement therapy, acute lung injury, acute respiratory distress syndrome*

Downloaded via PURDUE UNIV on April 5, 2024 at 21:53:37 (UTC).
See https://pubs.acs.org/sharingguidelines for options on how to legitimately share published articles.

1. INTRODUCTION

The successful treatment of premature infants suffering from severe respiratory distress using lung surfactant replacement therapy (SRT) has demonstrated the possibility of improving health outcomes by supplying exogenous lung surfactants;[1] however, the scope of SRT has not yet been successfully extended to adults suffering from acute respiratory distress syndrome (ARDS).[2] Viral infections, such as COVID-19, direct lung injury, gastric aspiration, sepsis, and inhalation of toxins, all can lead to the development of ARDS, which is characterized by the permeability of the alveolar membrane leading to severe hypoxia.[3] One of the harmful consequences of alveolar permeability is the dysfunction of the native lung surfactant, which coats the alveoli air−water interface, due to the influx of surface-active proteins and phospholipases (which degrade phospholipids).[4] The disruption of phospholipid-based surfactant films, which are the current state of the art for SRT, by surface-active proteins and phospholipases is thought to have contributed significantly to the lack of success of past SRT ARDS trials.[5] Therefore, we are exploring the use of a fundamentally different surfactant material composed of a biocompatible block copolymer to help address the current high mortality rates (40%) for ARDS patients.[6]

The polymer lung surfactant (PLS) formulation, composed of biocompatible poly(styrene-*block*-ethylene glycol) (PS-PEG), has several proposed advantages over conventional animal-derived phospholipid-based surfactants as depicted in Figure 1. Lipid surfactants are a multicomponent system that work in tandem to stabilize the alveoli during breathing. When the alveoli area is reduced during exhalation, less surface-active lipid components are displaced from the interface and are subsequently reabsorbed during inhalation (with the help of surfactant proteins),[7] making the lipid monolayer partially soluble and more susceptible to deactivation by proteins present in the subphase. In contrast, the high hydrophobicity of the PS core and the hydrophilic PEG brush layer combine to form an insoluble monolayer that is protected from interactions with surface-active proteins. Evidence for this has been given previously by demonstrating the superior surface-tension-lowering abilities of the PLS compared to exogenous surfactants when in the presence of a surface-active protein, serum albumin.[8] The superior surface-tension-lowering properties also translated to improved biomechanical function for mice receiving the PLS treatment compared to those receiving conventional animal-derived surfactants when tested immediately after surfactant instillation in a mouse model of lung injury.[8] Furthermore, no symptoms of toxicity were observed for the mice receiving PLS after 14 days as determined by body weight measurements, histological analysis of lungs, and cytokine levels in the bronchoalveolar lavage (BAL) fluid.[8]

Received: January 13, 2023
Accepted: March 30, 2023
Published: April 20, 2023

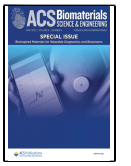

© 2023 American Chemical Society

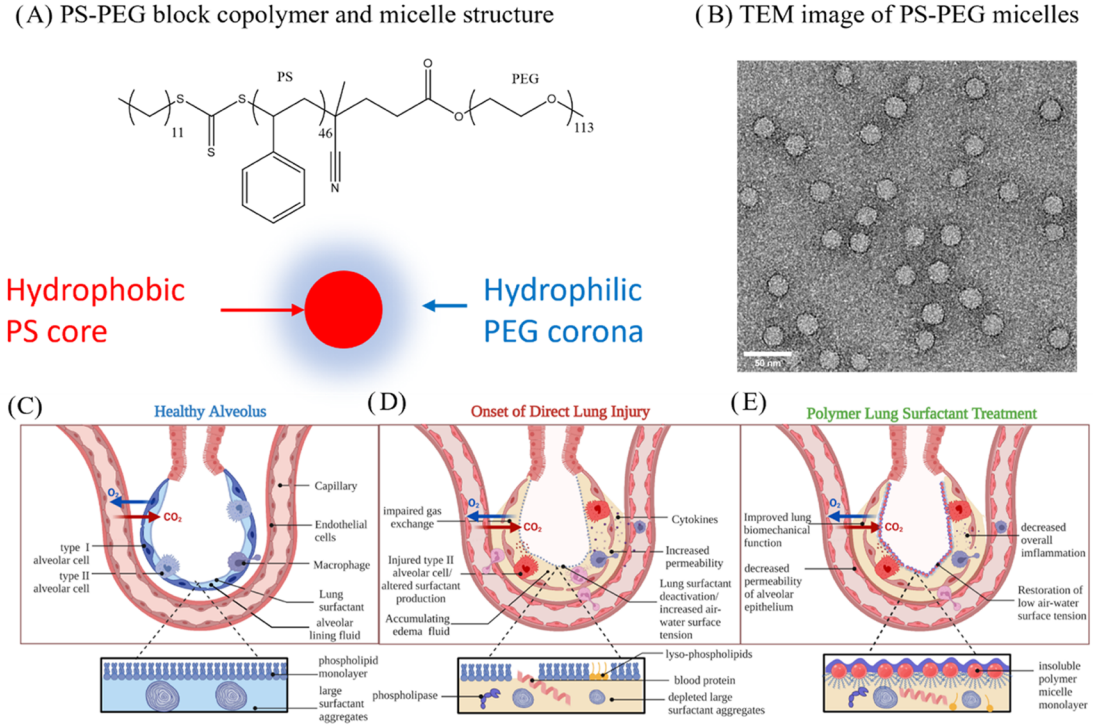

Figure 1. Overview of the design of the novel polymer lung surfactant therapy. (A) Structure of RAFT synthesized PS-PEG-OCH_3 block copolymer and the corresponding micelle structure. (B) TEM image of PS-PEG-OCH_3 micelle. (C) Overview of the structure of healthy alveolus. (D) Overview of symptoms that arise during direct lung injury, including the deactivation of the native lung surfactant by infiltrates to the alveolar space. (E) Schematic of polymer lung surfactant treatment. Alveoli cartoons were adapted from "SARS-CoV-2: what we know about its effects on respiration", by BioRender.com.

This paper provides an indepth study of the in vivo efficacy of PLS treatment in mouse models of lung injury induced by acid or lipopolysaccharide (LPS) aspiration. Specifically, the effect of PLS on the permeability of the alveolar membrane, health of lung tissue, levels of inflammation and hypoxia markers, and the native surfactant phospholipid recovery and composition following lung injury are analyzed up to 53 h post injury. The results provide evidence that PLS not only improves the biomechanical function of injured lungs but also helps mitigate the severity of overall lung injury as shown through several markers of lung health. Given the promising PLS efficacy results, other factors for the development of PLS are examined; namely, the long-term safety and stability of the PLS liquid suspension and the liquid distribution following pharyngeal administration are discussed.

2. MATERIALS AND METHODS

2.1. Animals. C57BL/6 mice (8−12 weeks old, female) were used. All procedures used were approved by the University Committee of Use and Care of Animals (UCUCA) of the University of Michigan at Ann Arbor (Protocol #PRO00009878) and by the Purdue University Institutional Animal Care and Use Committee (PACUC) (Protocol #1112000342) and comply with state and federal/NIH requirements.

2.2. Administration of Anesthetic, Analgesic, and Resuscitation. Animals were anesthetized by intraperitoneal (i.p.) injection of ketamine (80−120 mg/kg body weight) and xylazine (5−10 mg/kg body weight) or isoflurane inhalation. Systemic analgesics were not used because of their effects on the immune/inflammatory system. Animals were humanely euthanized in severe respiratory distress beyond 53 h.[9]

2.3. Murine Model of Gastric Acid Aspiration-Induced Lung Injury. The acid component of gastric aspirates was modeled with strong HCl. Under anesthesia, mice were injected with 30 μL of acid (HCl in normal saline (NS), pH 1.25) or NS (pH 5.3, vehicle control) by deep oral pharyngeal injection.[10] For pharyngeal injection, mice were placed on a custom-designed angled platform with their incisors hung on a wire. The tongue was pulled out of the mouse using forceps, and the liquid was directly dropped into the opening of the trachea using a micropipette. Mice were left to naturally recover from anesthesia.[11]

2.4. Murine Model of LPS-Induced Lung Injury. Mice were administered 50 μg/50 μL of *Escherichia coli* LPS (O111:B4) (Sigma-Aldrich, St. Louis, MO) by deep oral pharyngeal injection under isoflurane anesthesia. Animals were allowed to recover spontaneously.[9]

2.5. Polymer Lung Surfactant (PLS) Administration. At a designated time (typically, at 5 h) following the acid/LPS insult, 4 mL/kg of the PLS (PS-PEG micelle) solution (0.6 mg/mL in NS) was instilled into the mouse lungs by deep oral pharyngeal injection under isoflurane anesthesia.[12]

2.6. Bronchoalveolar Lavage (BAL) Fluid Collection. At the conclusion of a study, BAL fluids were collected by injecting and recovering two aliquots of 0.6 mL of ice-chilled phosphate-buffered saline (PBS) from each mouse. The two aliquots were combined and centrifuged at 150*g* at 4 °C for 10 min to remove cells and particles.[11]

2.7. Albumin Concentrations in BAL Fluids. Albumin concentrations in cell-free BAL fluids were measured by ELISA using polyclonal rabbit anti-mouse albumin antibody (1:1000, A90-135, Bethyl Laboratories, Inc.) and HRP-labeled goat anti-rabbit IgG (1:5000, A90-134P, Bethyl Laboratories, Inc.).[9,11]

2.8. Determination of Cytokine Levels in BAL Fluids and Lungs. Soluble concentrations of IL-1β, IL-6, MIP-2, KC, and MPO in cell-free BAL fluids and lungs following lung injury were determined using ELISA. Antibody pairs (capture and biotinylated reporter antibodies) and recombinant cytokines were purchased from R&D Systems.[11]

2.9. TaqMan Quantitative Polymerase Chain Reaction (qPCR). Total RNA was prepared from whole-lung lysates using an

https://doi.org/10.1021/acsbiomaterials.3c00061
ACS Biomater. Sci. Eng. 2023, 9, 2716−2730

RNeasy mini kit (Qiagen, Valencia, CA/Germantown, MD) following the manufacturer's protocol. 1 μg of the RNA was reverse-transcribed into cDNA using MMLV reverse transcriptase (Invitrogen, Carlsbad, CA). The cDNA was amplified by real-time TaqMan qPCR using an ABI Prism 7700 Sequence Detection System (Applied Biosystems, Foster City, CA). GAPDH was analyzed as an internal control. TaqMan gene expression reagents were used to determine the HIF1-α and VEGF-A levels (Applied Biosystems, Foster City, CA). qPCR data were expressed as fold change in transcript expression determined using software provided by Applied Biosystems.[9,11]

2.10. Histopathology. Formalin-fixed, paraffin-embedded lung tissues were sectioned and stained with hematoxylin and eosin (H&E). An experienced pathologist blindly evaluated H&E slides for indications of interstitial inflammatory cell infiltration, intra-alveolar hemorrhage, alveolar wall thickening, and pulmonary septal edema.[9] The pathology score was calculated semiquantitatively where the degree of injury was scored based on the following: no injury = 1, injury to 25% of the field = 2, injury to 50% of the field = 3, injury to 75% of the field = 4, and diffuse injury = 5.[13] To quantify neutrophils, five regions of H&E slides were analyzed under a high-magnification microscope, and the number of neutrophils were counted per high power field (HPF).

2.11. Closed-Chest Pressure−Volume (PV) Analysis. Pulmonary respiratory mechanics were measured postmortem, i.e., immediately after a blood sample was collected and the mouse was further exsanguinated by transection of the abdominal inferior vena cava. An 18-gauge metallic cannula was inserted into the trachea through a midline cervical exposure. The mouse was then connected to a SCIREQ Flexivent (Montreal, QC, Canada), a small animal ventilator with which PV data were acquired during ventilation. Parameter settings were as follows: tidal volume = 10 mL/kg; respiratory rate = 150 breaths/min; and positive end-expiratory pressure = 2 cm H_2O. Using a ramp-style volume-driven (PVrV) maneuver, the PV curve and quasi-static compliance were measured during an inflation−deflation cycle.[9]

2.12. Lipidomics of Large Surfactant Aggregates. Large surfactant aggregates were isolated by centrifugation of 200 μL of cell-free BAL fluid at 12,000*g* for 30 min. After isolating large aggregates, the phospholipids were separated using the Bligh and Dyer extraction method.[14] Once solid phospholipids were dried, the solids were dissolved into 200 μL of 3:6.65:0.35 acrylonitrile (ACN) + methanol (MeOH) + 300 mM ammonium acetate (NH_4Ac) solution and subsequently diluted 40× in the same solvent to make the final solution analyzed using multiple reaction monitoring (MRM) mass spectrometry (MS).[15] MRM MS relies on direct sample injection and functional group monitoring using neutral loss and precursor MS scans. A micro-autosampler (G1377A) was used to deliver 8 μL/sample by flow injection to the ionization source of an Agilent 6410 QQQ mass spectrometer (Agilent Technologies, Santa Clara, CA). The capillary pump of the autosampler operated with a pressure of 150 bar and a 10 μL/min flow. The capillary voltage was 3.5−5 kV, and the gas flow was 5.1 L/min at 300 °C The phosphatidylcholine (PC) and lysophosphatidylcholine (LysoPC) amounts were analyzed by spiking the samples with lipid standards (Avanti Polar Lipids). Absolute and relative amounts of six PC lipids and one LysoPC lipid were analyzed.

2.13. Live Animal Lung Imaging by X-ray Computed Tomography (CT). X-ray CT was used to determine three-dimensional (3D) distributions of instilled liquid in the lungs with 4−5 μm spatial resolution. To measure liquid distribution and clearance, iohexol, a commercially available iodine CT contrast agent, was added to PLS (0.6 mg/mL) at a concentration of 50 mgI/mL. C57BL/6 mice were administered PLS + iohexol solution at a dose volume of 4 mL/kg body weight, anesthetized using isoflurane, and placed inside a PerkinElmer Quantum GX microCT scanner. Isoflurane was continuously administered during the scan. The imaging parameters were set as follows: voltage = 90 kV; current = 88 μA; field of view = 25 mm, scan time = 2 min, and pixel size = 50 μm. CT scans were obtained while mice were under isoflurane anesthesia.

2.14. Poly(Styrene-*block*-Ethylene Glycol) (PS-PEG) Synthesis. PS-PEG was synthesized via reversible addition−fragmentation chain transfer (RAFT) polymerization. 4-Cyano-4-[(dodecylsulfanylthiocarbonyl)sulfanyl] pentanoic acid (Sigma-Aldrich) was used as the RAFT agent. First, the RAFT agent was conjugated to purified poly(ethylene glycol) monomethyl ether (PEG-OH, M_n = 5000 g/mol, Sigma-Aldrich) by Steglich esterification.[16] The PEG-OH (1 g, 0.2 mmol), the RAFT agent (161.4 mg, 0.4 mmol), and 4-dimethylamino pyridine (4.89 mg, 0.04 mmol, Sigma-Aldrich) were mixed in 10 mL of dichloromethane (Sigma-Aldrich) and kept under magnetic stirring at 0 °C. A separately prepared dicyclohexylcarbodiimide (82.5 mg, 0.4 mmol) solution in dichloromethane (5 mL) was added dropwise to the above mixture and allowed to undergo reaction for 5 min at 0 °C and then for 3 h at 20 °C to produce "PEG-RAFT". The as-synthesized PEG-RAFT product was first filtered through a filter paper to remove the insoluble urea byproduct and then further purified by precipitation in hexane twice. The RAFT polymerization reaction was performed at 70 °C by mixing the PEG-RAFT, inhibitor-free styrene (Sigma-Aldrich), and a free radical initiator, azobisisobutyronitrile (Sigma-Aldrich) in dioxane (Sigma-Aldrich). The resulting PS-PEG products were precipitated twice in hexane and dried under vacuum. Two batches of PS-PEG were used in this study having molecular characteristics of PS(4.4 kDa)−PEG(5.0 kDa) and PS(4.8 kDa)−PEG(5.0 kDa).

2.15. Polymer Micelle Formulation. Since PS-PEG is a highly amphiphilic block copolymer (BCP), the polymer cannot be directly dissolved in water. Therefore, a solvent exchange procedure must be used to formulate PS-PEG micelle solutions. Two different procedures, the syringe pump method[8] and equilibration nano precipitation (ENP),[17] have been used to prepare PS-PEG micelle solutions for animal studies; however, both procedures produced micelle batches with matching size and surface-mechanical properties. ENP has become the method of choice due to its ease of setup and superb reproducibility. The two methods are as follows.

(a) The syringe pump method starts with dissolving 50 mg of the BCP in 1 mL of acetone. Then, a syringe pump is used to add 9 mL of water at a flow rate of 0.0125 mL/min while the polymer solution is under vigorous stirring. The solution was kept under stirring for 24 h. The solution was then dialyzed using 50 kDa dialysis against 1 L of bulk Milli-Q water for 24 h, changing the bulk reservoir five times. For animal experiments, the solution was diluted to a final concentration of 0.6 mg/mL and salt was added so that the micelles were suspended in normal saline.

(b) ENP begins by dissolving the BCP in an acetone/water mixture (60 vol % water for this study) at a concentration of 10 mg/mL. The solution was kept under gentle agitation overnight to allow the system to approach the equilibrium state. 50 kDa dialysis tubing was used to remove the acetone and achieve aqueous solutions. The solutions were dialyzed against 1 L of bulk Milli-Q water for 24 h, changing the bulk reservoir five times. For animal experiments, the solution was diluted to a final concentration of 0.6 mg/mL, and salt was added so that the micelles were suspended in normal saline.

2.16. Polymer Micelle Characterization Studies. The hydrodynamic diameters of the PS-PEG micelles were measured by dynamic light scattering (DLS) using a Brookhaven ZetaPALS instrument. The scattering intensities were measured using a 659 nm laser at a scattering angle of 90°. The hydrodynamic diameters were calculated from the measured diffusion coefficients using the Stokes−-Einstein equation. For DLS measurements, the samples were diluted to guarantee single scattering and were filtered with 0.45 μm syringe filters to remove contaminants. Formulations used in mouse studies had aqueous hydrodynamic diameters in the range of 28−30 nm and core diameters in the range of 20−22 nm. Representative dynamic light scattering (DLS) size histogram is shown in Figure S1.

2.17. Surface Pressure−Area Isotherms. A KSV 5000 Langmuir trough (54 cm × 15 cm, 1.4 L subphase volume) with

https://doi.org/10.1021/acsbiomaterials.3c00061
ACS Biomater. Sci. Eng. 2023, 9, 2716−2730

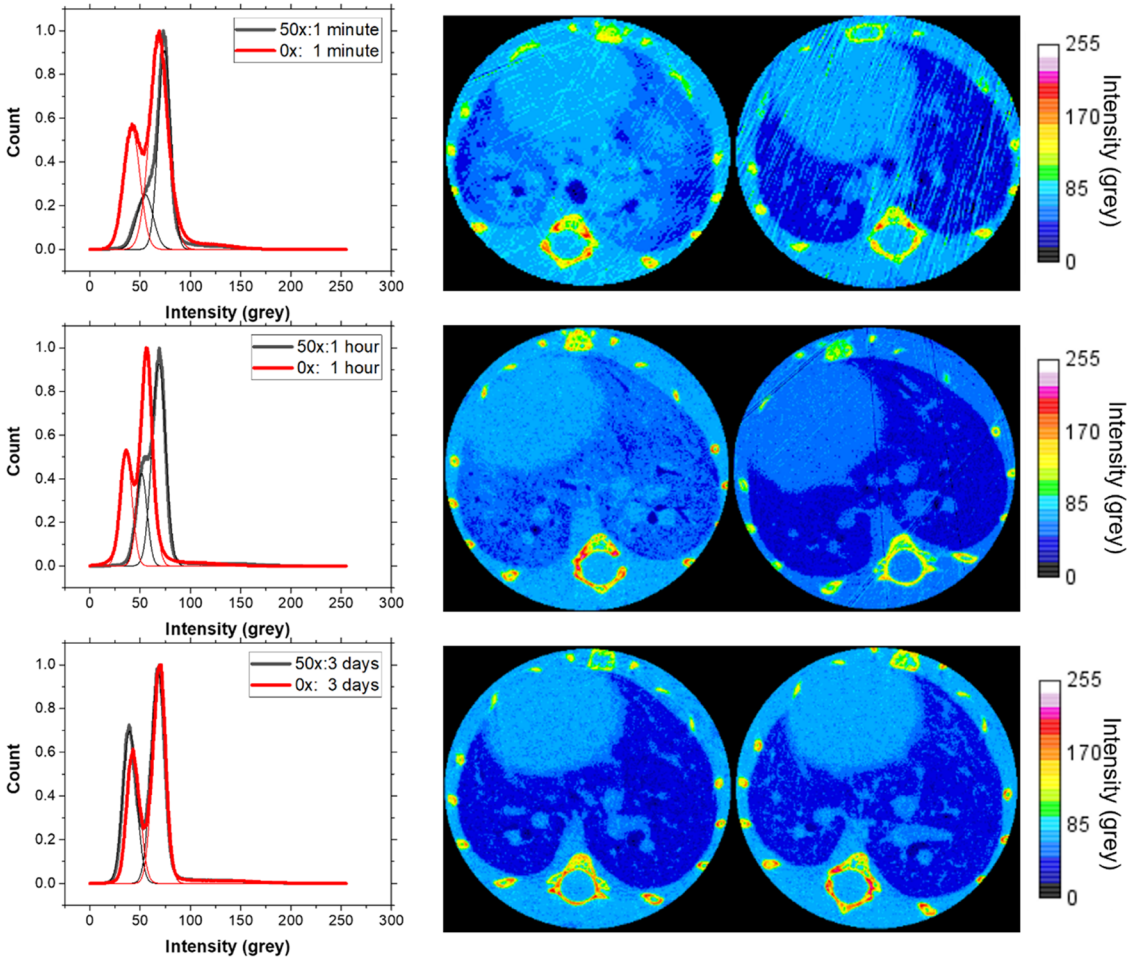

Figure 2. Liquid distribution and clearance of PLS with added water-soluble contrast medium. (Left) Population distribution of intensity values for whole computed tomography (CT) stacks for saline only ("0×") and 50 mgI/mL ("50×"). The thinner lines correspond to Gaussian fits of the two peaks. (Right) Side-by-side two-dimensional (2D) slices from CT scans of mice chest cavities. The far right images are from mice receiving 0× instillation and the left image is the 50× case.

two symmetric barriers was used for surface pressure−area isotherm measurements. The trough had a heating/cooling water jacket embedded underneath, which was connected to a circulating water bath. The temperature of the water subphase was monitored using a thermocouple within 0.1 °C accuracy; all measurements were conducted at 25 °C. Milli-Q-purified water (18 MΩ·cm resistivity) was used as the subphase solvent that had a surface tension of 72 mN/m at 25 °C. Compression was done at a rate of 3 mm/min. Formulations for mouse studies were verified to produce surface pressures greater than 60 mN/m.

2.18. Statistics. Data are expressed as the mean ± standard error of mean (SEM) in all figures. Statistical differences between injury only and injury with PLS treatment were analyzed using a two-tailed, unpaired *t*-test. Significance levels are defined as $*p < 0.05$, $**p < 0.01$, $***p < 0.001$, and $****p < 0.0001$.

3. RESULTS

3.1. PLS Liquid Delivery and Clearance Following Pharyngeal Aspiration. The success of an SRT treatment is dependent upon the surfactant effectively reaching the alveoli. Different administration methods have been developed to deliver surfactant to the lungs including both invasive methods, such as intratracheal instillation, and noninvasive methods, such as aerosolization. In the following efficacy studies, the pharyngeal administration (tongue-pull) method was used as it is noninvasive and prevents factors such as mechanical ventilation from contributing to lung injury. However, since pharyngeal methods do not deliver the surfactant deep into airways, there is a higher likelihood of surfactant not effectively reaching the distal airways. A previous study of the pulmonary pharmacokinetics of pharyngeal-administered PLS at therapeutic dosage demonstrated that the PLS is primarily cleared by the mucociliary escalator of the conductive airways, and a small percentage actually makes it to the alveoli.[12] The amount that does reach the alveoli remains in the lungs for around 16 days.[12] One possible reason for the low amount reaching the alveoli is due to poor liquid distribution in the lungs following pharyngeal administration. A simulation study found that the instilled liquid transport of surfactants in the pulmonary airways is determined by parameters such as dose volume, flow rate, liquid viscosity, airway bifurcation morphology, and body positioning.[18] To demonstrate the liquid spreading and clearance of the PLS suspension at the concentration used in efficacy studies (0.6 mg/mL) in the lungs following pharyngeal administration, a computed tomography (CT) study was done using an added water-soluble contrast agent (PLS + iohexol).

The PLS + iohexol formulation was instilled into the lungs, and CT scans were taken at various time points. Figure 2 shows cross-sectional CT slices of the chest cavity of mice receiving instillation of PLS + iohexol in saline (left) and saline only (right) at 1 min, 1, and 72 h post instillation. In the CT

https://doi.org/10.1021/acsbiomaterials.3c00061
ACS Biomater. Sci. Eng. 2023, 9, 2716−2730

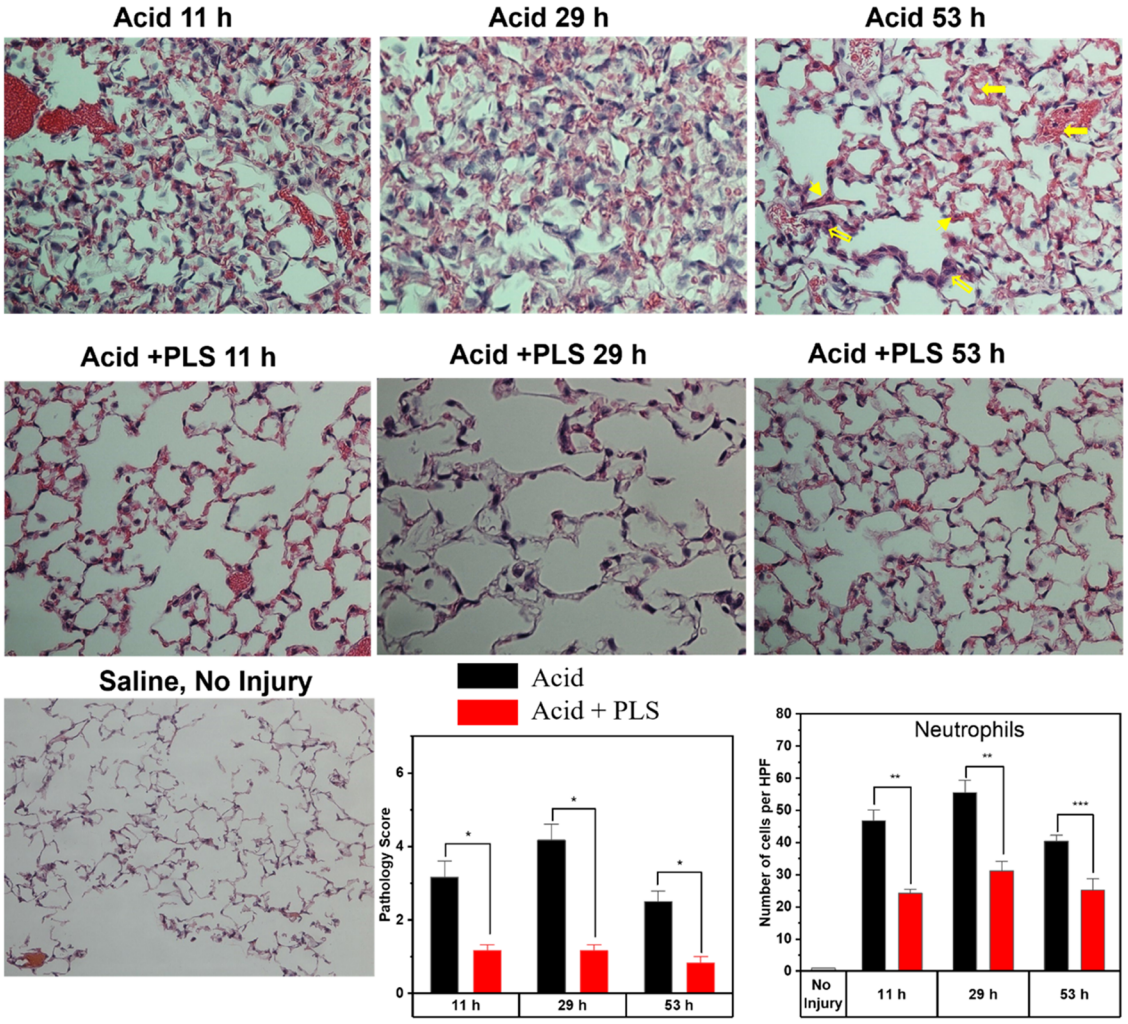

Figure 3. Hematoxylin-and-eosin (H&E)-stained sections of acid-aspirated lungs (original magnification ×40) and noninjured lung (original magnification ×20). The pathology score was calculated semiquantitatively where the degree of injury was scored based on the following: no injury = 1, injury to 25% of the field = 2, injury to 50% of the field = 3, injury to 75% of the field = 4, and diffuse injury = 5. Examples of lung injury pathologies are labeled in the Acid 53 h image where the open arrow represents interstitial inflammatory cell infiltration (increase in the density of nuclei (stained dark blue)), filled arrows represent pulmonary edema (increase in edema fluid (stained pink)), and filled arrowhead represents alveolar wall thickening. To quantify neutrophils, five regions of H&E slides were analyzed under a high-magnification microscope and the number of neutrophils were counted per high power field (HPF). WT C57BL/6 mice were treated with 30 μL of acid (NS + HCl, pH 1.25) using pharyngeal administration. 90 μL of PLS (0.6 mg/mL in 0.9% saline) using pharyngeal administration at 5 h post acid treatment. Mice were allowed to recover spontaneously afterward and sacrificed at 11, 29, and 53 h following acid insult (N = 3). *p < 0.05.

images, the dark blue areas represent the empty air space in the lungs, the lighter blue spots inside the lungs are blood vessels, the large light blue circular region is the heart, and the bright spots encircling the lungs are bones from the ribs and chest. Pixel intensity normalized population distributions for whole CT stacks are also plotted for each time point. In this population distribution, the peak at lower gray values is from the air-filled lung space, and the peak at higher gray is from the blood vessels and tissue inside and surrounding the lungs. At 1 min post injection, there appear lighter regions that are caused by the iohexol-containing liquid coating the lungs. At 1 h, the liquid begins to be transported out of the lung space, causing a reemergence of the air space peak in the population distribution. After 3 days, the air space has been completely recovered, and the CT images and intensity population distributions are nearly identical for both cases. By comparing the area ratios of the air space peak and the tissue/blood vessel peak for each time point, the percentage of iohexol that has left the lung in 1 h is calculated to be 17.5%. An estimation of the percentage of the lung covered by the liquid in 1 min after instillation could also be made (≅60.0%) by assuming that the ratio at 3 days corresponds to no liquid covering the lungs. Therefore, although the delivery of PLS to alveoli needs to be further improved, pharyngeal administration shows to deliver a significant amount of administered liquid into airways.

3.2. PLS Treatment in Acid-Induced Lung Injury in Mice. The aspiration of gastric contents is one common risk factor for developing ARDS.[19] A widely used model for gastric aspiration is the instillation of HCl into the trachea, which mimics the low pH properties of gastric fluids. ALI by low pH aspiration is neutrophil-dependent and leads to injury of airways and alveolar epithelium.[20] Investigations of acid-induced injury models, like the one used in this paper, have shown that instillation of HCl initiates lung injury either by direct chemical burn and/or stimulation of afferent nerves. After several hours, the second phase of injury begins in which

https://doi.org/10.1021/acsbiomaterials.3c00061
ACS Biomater. Sci. Eng. 2023, 9, 2716−2730

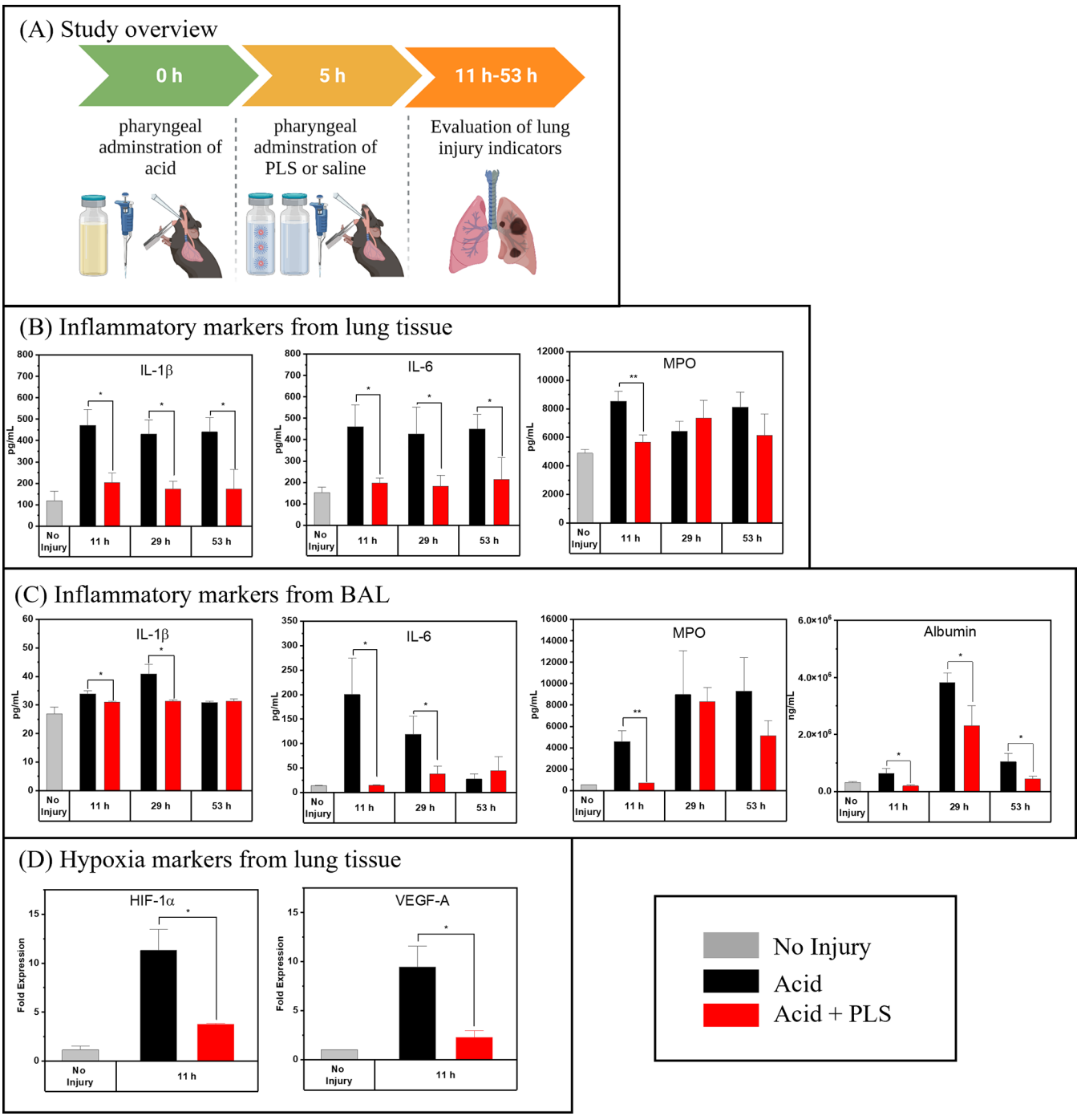

Figure 4. Reduction in inflammatory markers after PLS treatment in the acid-induced injury model. (A) Overview of the acid-injury model (created with BioRender.com). Effects of PLS on albumin (serum protein), interleukin-1β (IL-1β) (proinflammatory cytokine), interleukin-6 (IL-6) (proinflammatory cytokine), and myeloperoxidase (MPO) (inflammatory enzyme) levels in (B) bronchoalveolar lavage (BAL) fluids from acid-aspirated lungs and (C) lung tissue. (D) Effect of PLS on the levels of hypoxia-inducible factor-1α (HIF-1α) (endogenous hypoxia marker) and vascular endothelial growth factor-A (VEGF-A) (angiogenesis marker upregulated by hypoxia) levels in acid-aspirated lungs from real-time PCR of entire lungs (N = 3) C57BL/6 mice were treated with 30 μL of pharyngeal-administered acid (normal saline (NS) + HCl, pH 1.25). 90 μL of PLS (0.6 mg/mL in 0.9% saline) was pharyngeally administered at 5 h post acid treatment. Mice were allowed to recover spontaneously afterward and sacrificed at 11, 29, and 53 h following acid insult (N = 6). *p < 0.05 and **p < 0.01.

the inflammatory response, resulting in neutrophilic infiltration, leads to increased alveolar permeability and subsequent surfactant deactivation. Studies in mice have shown that the transient inflammatory phase occurs for a longer time period peaking around 24 h post acid instillation.[21] The prolonged worsening of symptoms is thought to be in part due to the dysfunction of the native surfactant and the subsequent collapse and damage of the alveolar epithelium. Therefore, PLS was administered to acid-injured mice to analyze if using a properly designed surfactant replacement can reduce the symptoms of acute acid injury by restoring the low-surface-tension conditions required for proper alveolar function.

Histopathological analysis was conducted for mice lungs after instillation of acid with and without PLS treatment (at 5 h

https://doi.org/10.1021/acsbiomaterials.3c00061
ACS Biomater. Sci. Eng. 2023, 9, 2716−2730

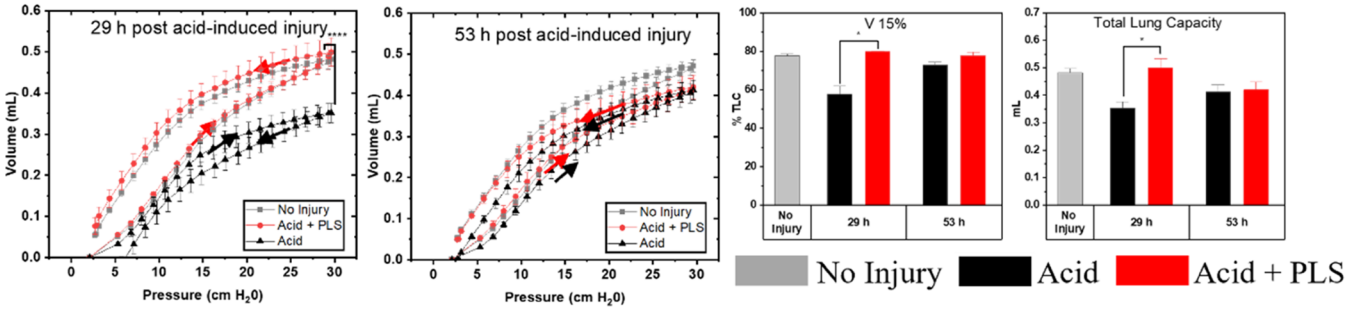

Figure 5. Measurements of lung pressure−volume (PV) mechanics after PLS treatment in the acid-induced injury model. Effects of PLS on closed-chest pressure−volume curves along with the corresponding total lung capacity (TLC) and percentage lung volume at 15 cm H_2O (V 15%) (N = 4). Error bars represent ±SEM. TLC corresponds to lung volume at a pressure of 30 cm H_2O. V 15% is the percentage of TLC at 15 cm H_2O during deflation. WT C57BL/6 mice were treated with 30 μL of pharyngeal acid (normal saline (NS) + HCl, pH 1.25). 90 μL of PLS (0.6 mg/mL in 0.9% saline) was pharyngeally administered at 5 h post acid treatment. Mice were allowed to recover spontaneously afterward and sacrificed at specified time points following acid insult (N = 5). *p < 0.05, **p < 0.01, ***p < 0.001, and ****p < 0.0001.

post acid instillation) at 11, 29, and 53 h after acid instillation. Lung tissues were sectioned and stained with hematoxylin and eosin (H&E); representative images of H&E-stained lung sections are shown in Figure 3 along with the pathology score and neutrophil counts. The pathology score was calculated semiquantitatively where the degree of injury was scored based on the following: no injury = 1, injury to 25% of the field = 2, injury to 50% of the field = 3, injury to 75% of the field = 4, and diffuse injury = 5. Lung injury for the acid-injury model is characterized primarily by interstitial inflammatory cell infiltration, pulmonary edema, and alveolar wall thickening, and examples of injuries are labeled in Acid 53 h image where open arrows represent interstitial neutrophil infiltration (increase in the density of nuclei (stained dark blue)), filled arrows represent pulmonary edema (increase in edema fluid (stained pink)), and filled arrowheads represent alveolar wall thickening. For the acid-only case, the peak of injury occurred at 29 h with there being a significant presence of diffusive alveolar damage that is characterized by interstitial and airspace edema and inflammatory cell infiltrates. The Acid + PLS images clearly show that PLS mitigates the progression of the diffusive alveolar damage symptoms as lung images display only minor occurrences of lung injury that is reflected in the significantly lower histopathologic score and neutrophil counts of PLS-treated animals at each time point.

The extent of permeability and inflammation after acid-induced injury were analyzed by determining the levels of albumin in BAL as well as levels of inflammatory markers in BAL and lung tissues. Albumin is a surface-active blood protein that can disrupt the proper functioning of the native lung surfactant through competitive adsorption to the air−water interface.[22] During lung inflammation, an increase in alveolar epithelial permeability leads to albumin leakage into the alveolar space. The results shown in Figure 4 demonstrate that treatment with PLS led to a significant reduction in the level of albumin in the BAL fluid in all three time points post acid-induced injury which indicates mitigation of epithelial permeability. Also, in BAL for the Acid + PLS treatment group, there was a significant reduction in the interleukins (proinflammatory cytokines) IL-1β and IL-6 at 11 and 29 h post acid injury and a significant reduction in the inflammatory enzyme myeloperoxidase (MPO) at 11 h post injury compared to the acid-only group. IL-6 is a cytokine that is produced by inflammatory cells (e.g., macrophages and neutrophils), as well as by lung epithelial cells, and has been positively associated with inflammatory lung diseases.[23] IL-1β has been shown to be responsible for the recruitment of neutrophils to the alveoli.[24] MPO is secreted by neutrophils after undergoing secondary necrosis and is suggested to cause damage to lung epithelial cells.[25] In measurements of lung tissue for the Acid + PLS group, the levels of IL-1β and IL-6 were significantly reduced at all three time points post injury, and MPO level was significantly reduced at 11 h post acid-induced injury compared to the acid-only group. Overall, PLS treatment demonstrated the ability to lower both alveolar permeability and the level of multiple proinflammatory markers after acid-induced injury.

Acid-induced injury has been shown to cause a decrease in lung compliance and subsequent hypoxia due to, in part, lung surfactant dysfunction.[26] Therefore, the levels of hypoxic markers (Figure 4D) and lung pressure−volume (PV) curves (Figure 5) after acid-induced injury with and without PLS treatment were measured. The levels of hypoxic markers were measured using real-time PCR on the whole-lung tissue 11 h after acid instillation to detect differences in gene expression between treatment and nontreatment groups. The results given in Figure 4D show that PLS treatment led to a significantly lower expression of both hypoxia-inducible factor-1α (HIF-1α), an angiogenesis hypoxia marker, and vascular endothelial growth factor-A (VEGF-A), an angiogenesis marker upregulated by hypoxia. Since both of these genes are key mediators of adaptation to hypoxia,[27] the results indicate that PLS limited hypoxic conditions during the hours following acid instillation.

To test lung mechanics, lung pressure−volume (PV) curves of acid-injured lungs with and without PLS treatment were measured at 29 and 53 h after acid injury. Lung PV curves provide insight into the biomechanical function of the lung. As the surface tension within the lung increases, more pressure is required to generate the same increase in lung volume. Additionally, since surface tension contributes to the elastic recoil of lungs during exhalation, an increase in surface tension leads to a sharper decrease in volume with respect to pressure during exhalation (deflation).[28] In Figure 5, PV curves along with the total lung capacity (TLC), estimated by calculating the volume increase at a pressure of 30 cm H_2O, and the percentage of TLC of the volume at 15 cm H_2O deflation pressure (V 15%) are shown for treatment and nontreatment groups. The inflation PV curves for 29 h post injury demonstrate that PLS treatment leads to a significant increase in lung volumes at pressures greater than 15 cm H_2O

https://doi.org/10.1021/acsbiomaterials.3c00061
ACS Biomater. Sci. Eng. 2023, 9, 2716−2730

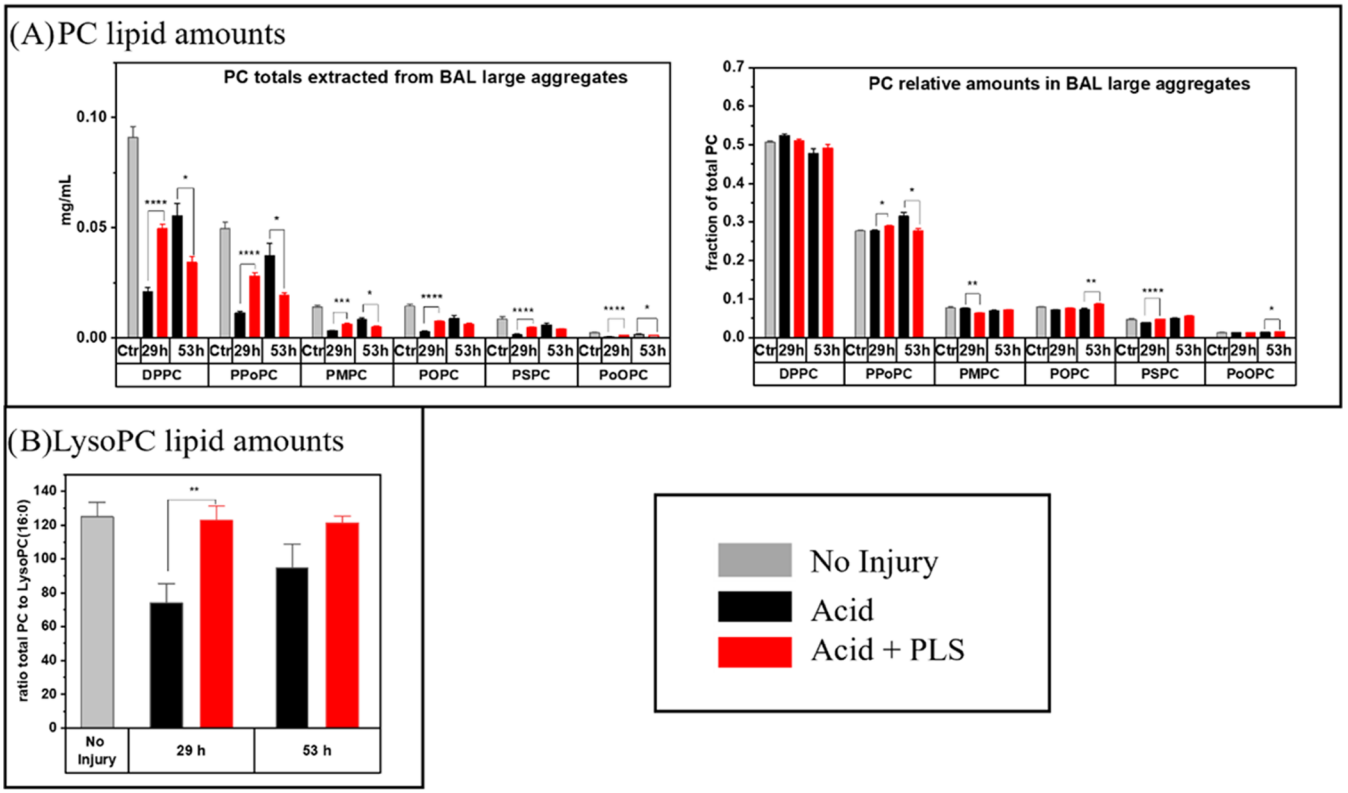

Figure 6. (A) Effects of PLS treatment on the amount and composition of large surfactant aggregates after acid-induced injury. (Left) Absolute and (middle) relative amounts of six phosphatidylcholine (PC) lipids in large surfactant aggregates extracted from the bronchoalveolar lavage (BAL) fluid. The specific lipids are dipalmitoyl-PC (DPPC), palmitoyl-palmitoleoyl-PC (PPoPC), palmitoyl-myristoyl-PC (PMPC), palmitoyl-oleoyl-PC (POPC), palmitoyl-stearoyl-PC (PSPC), and palmitoleoyl-oleoyl-PC (PoOPC). (B) Ratio of total PC amount to the amount of lysophosphatidylcholine (LysoPC) lipid LysoPC (16:0). Large surfactant aggregates were extracted from BAL by centrifuging at 12,000*g* for 30 min ($N = 5$). WT C57BL/6 mice were treated with 30 μL of pharyngeal acid (normal saline (NS) + HCl, pH 1.25). 90 μL of PLS (0.6 mg/mL in 0.9% saline) was pharyngeally administered at 5 h post acid treatment. Mice were allowed to recover spontaneously afterward and sacrificed at specified time points following acid insult. *$p < 0.05$, **$p < 0.01$, ***$p < 0.001$, and ****$p < 0.0001$.

compared to the nontreatment group. Also, the higher increase in volume at high pressures translates to a significantly greater TLC. Additionally, the PV deflation curves show that PLS treatment leads to a more gradual decrease in volume as pressure is decreased compared to the nontreatment group which is reflected in the significantly higher V 15% value. Both measurements are consistent with the idea that PLS restores the low air−water surface tension in the acutely injured lung as the PLS-treated lung expands more easily when inflated and recoils less vigorously when deflated. At 53 h after acid injury, the effects are less pronounced as the degree of injury is less severe at this time point. The results suggest that PLS treatment caused significant improvement in the lung biomechanical function by restoring low air−water surface tension at 29 h after injury when progression of injury reached its peak in severity, but the effects were not significant at 53 h when the injury status was less severe.

To analyze the effects of PLS on the composition of the native lung surfactant, a lipidomics mass spectrometry analysis was done on large aggregates from BAL, which contains the active ingredients of the lung surfactant,[29] to measure absolute and relative levels of six abundant phosphatidylcholine (PC) lipids in the lung surfactant that are DPPC (PC 32:0), PPoPC (PC 32:1), POPC (PC 34:1), PMPC/MPPC (PC 30:0), PSPC (PC 34:0), and PoOPC (PC 34:2). These lipids correspond to roughly 90% of PC lipids and 70% of total phospholipid content in the lung surfactant.[30] Additionally, the ratio of the total amount of the six aforementioned PC lipids to the amount of the most abundant lysophosphatidylcholine lipid (LysoPC 16:0), which has been shown to be produced via enzymatic degradation of PC lipids during lung inflammation,[31] was measured. The increase in the relative mass fraction of LysoPC has been shown to have negative impacts on the surface-mechanical behavior of the natural lung surfactant.[32] The lipidomics results (Figure 6) show that for the PLS group at 29 h post acid instillation (when injury symptoms are most severe), the values for the absolute amounts recovered from BAL large aggregates of all measured PC lipids and the ratio of PC lipids to LysoPC 16:0 were significantly greater than the acid-only group. However, at 53 h post acid instillation, the absolute amount of all but POPC and PSPC was greater for the acid-only group compared to the PLS group. Therefore, the PLS does not show the ability to restore the levels of large surfactant aggregates at the time points measured in this experiment. There were also significant differences between relative PC amounts for both 29 and 53 h post acid instillation; however, the magnitudes of the differences were minor compared to the absolute amounts. The results indicate that PLS mitigated the severity of reduction of the active surfactant in BAL and the degradation of PC to LysoPC at 29 h after acid injury, but PLS treatment did not promote the restoration of the active native surfactant amount at 53 h after acid injury.

3.3. PLS Treatment in LPS-Induced Lung Injury in Mice. Gram-negative bacteria, such as *E. coli*, have the

https://doi.org/10.1021/acsbiomaterials.3c00061
ACS Biomater. Sci. Eng. 2023, 9, 2716−2730

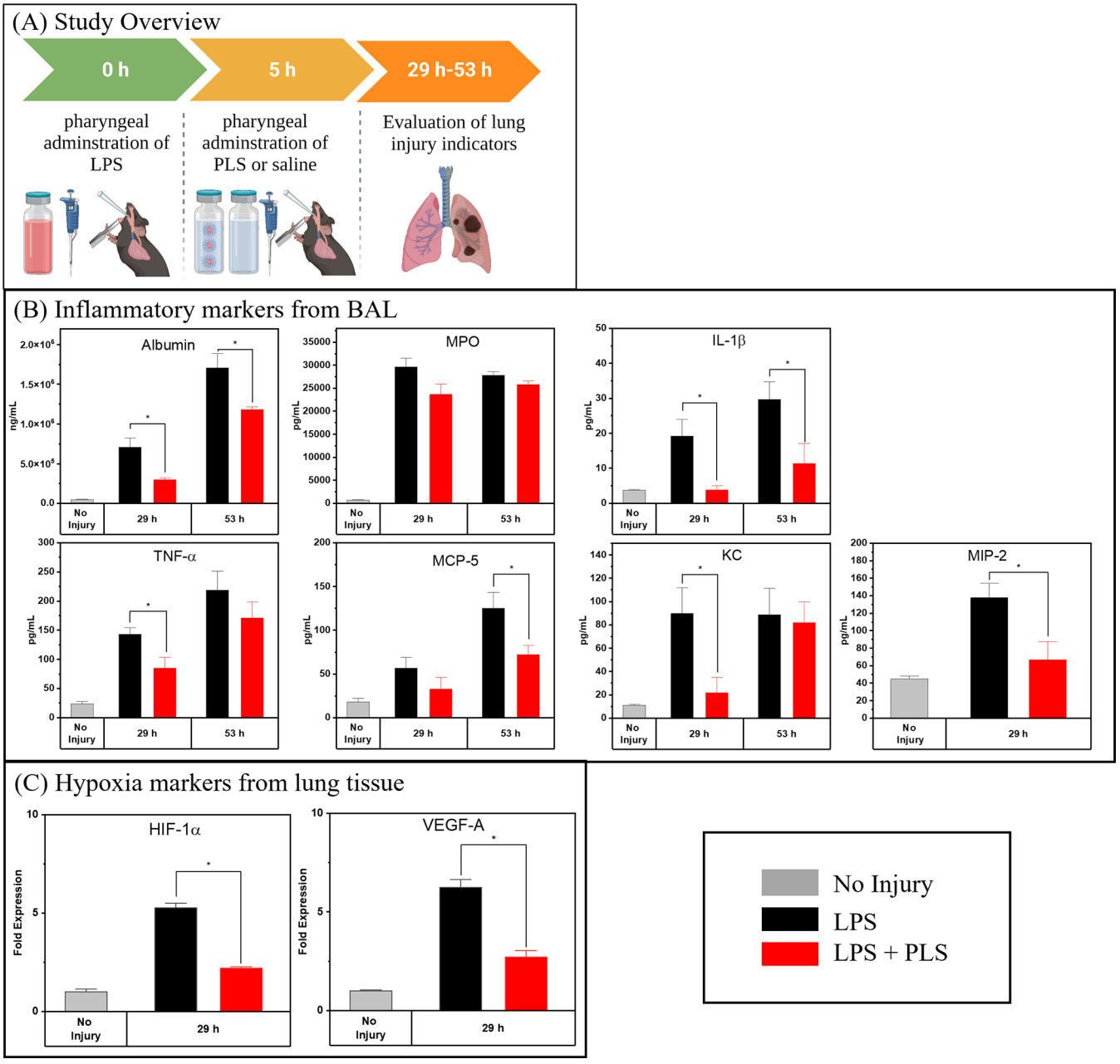

Figure 7. Improvement of various respiratory health markers after PLS treatment in LPS-induced injury model. (A) Overview of LPS injury model (created with BioRender.com). (B) Effects of PLS on albumin (serum protein), interleukin-1β (IL-1β) (proinflammatory cytokine), myeloperoxidase (MPO) (inflammatory enzyme), tumor necrosis factor-α (TNF-α) (proinflammatory cytokine), monocyte chemotactic protein-5 (MCP-5) (proinflammatory cytokine), keratinocyte chemoattractant (KC) (proinflammatory cytokine), and macrophage inflammatory protein-2 (MIP-2) (proinflammatory cytokine) levels in bronchoalveolar lavage (BAL) fluids from lungs with lipopolysaccharide (LPS)-induced injury (N = 5). (C) Effects of PLS on the levels of hypoxia-inducible factor-1α (HIF-1α) (endogenous hypoxia marker) and vascular endothelial growth factor-A (VEGF-A) (angiogenesis marker upregulated by hypoxia) levels in LPS-treated lungs from real-time PCR of entire lungs. *p < 0.05, **p < 0.01, and ***p < 0.001.

potential to induce sepsis shock through the release of an endotoxin, lipopolysaccharide (LPS), which is contained in their cell membranes.[33] The cascading inflammatory response accompanying the development of sepsis is a serious risk factor for the development of ARDS. Therefore, the instillation of LPS in the lungs is a common model for endotoxin-induced lung injury. Tracheal instillation of LPS leads to damage to the alveolar epithelium cells due to the recruitment of inflammatory cells.[33] Importantly, LPS is known to interact with alveolar type II (AT2) cells depleting and inactivating the natural lung surfactant.[33] Therefore, PLS was administered to mice following LPS administration, and various health markers were measured.

The extent of permeability and inflammation after LPS-induced injury was analyzed by determining the levels of albumin and inflammatory markers in BAL at 29 and 53 h after LPS administration (Figure 7). Like the acid-injury model, the PLS treatment led to a significant decrease in albumin levels in the BAL at both time points after injury, indicating a reduction in alveolar epithelial permeability. Additionally, IL-1β was

https://doi.org/10.1021/acsbiomaterials.3c00061
ACS Biomater. Sci. Eng. 2023, 9, 2716−2730

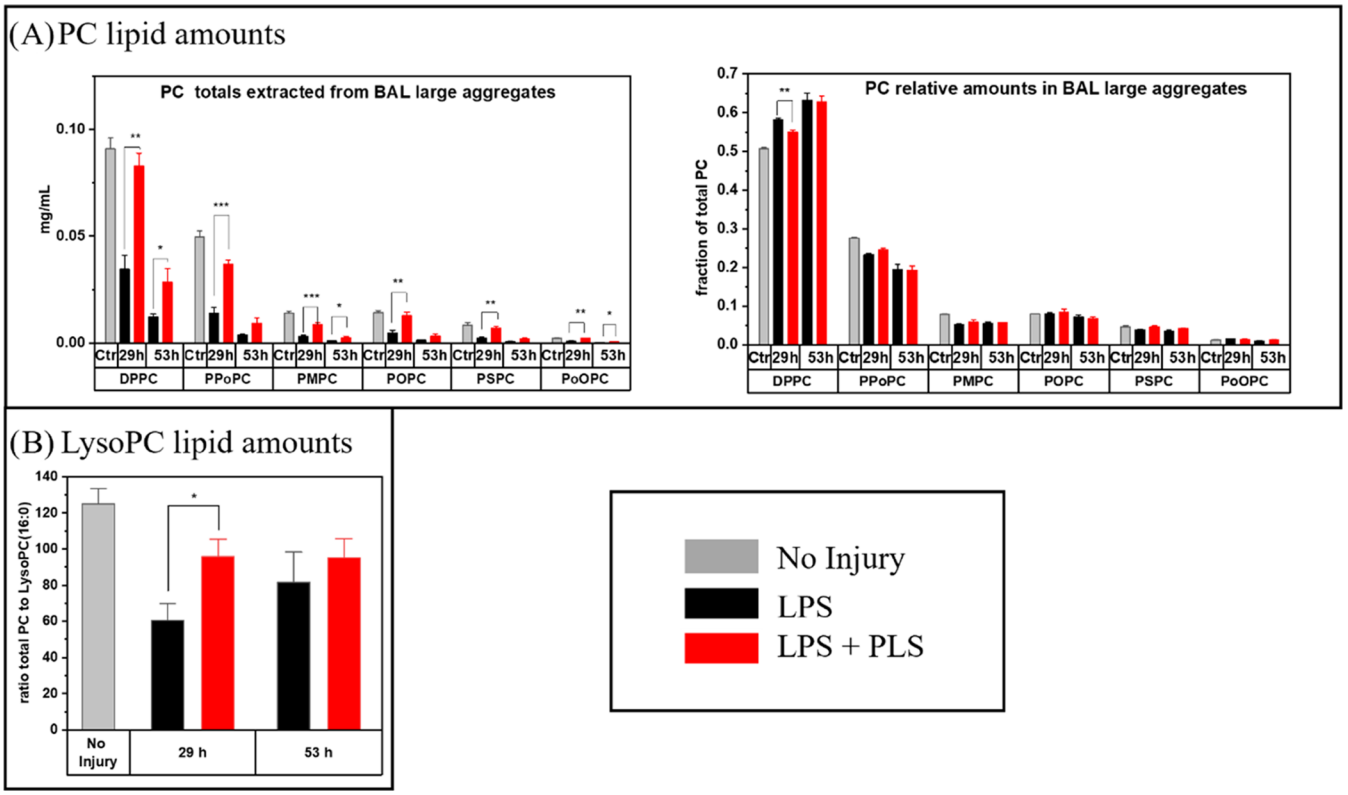

Figure 8. (A) Effects of PLS treatment on the amount and composition of large surfactant aggregates after LPS-induced injury. (Left) Absolute and (middle) relative amounts of six phosphatidylcholine (PC) lipids in large surfactant aggregates extracted from the bronchoalveolar lavage (BAL) fluid. The specific lipids are dipalmitoyl-PC (DPPC), palmitoyl-palmitoleoyl-PC (PPoPC), palmitoyl-myristoyl-PC (PMPC), palmitoyl-oleoyl-PC (POPC), palmitoyl-stearoyl-PC (PSPC), and palmitoleoyl-oleoyl-PC (PoOPC). (B) Ratio of total PC amount to the amount of lysophosphatidylcholine (LysoPC) lipid LysoPC (16:0). Large surfactant aggregates were extracted from BAL by centrifuging at 12,000*g* for 30 min ($N = 5$). WT C57BL/6 mice were treated with 50 μg of pharyngeally delivered LPS (normal saline (NS) + LPS). 90 μL of PLS (0.6 mg/mL in 0.9% saline) was pharyngeally administered at 5 h post LPS treatment. Mice were allowed to recover spontaneously afterward and sacrificed at 29 and 53 h following LPS insult ($N = 5$). *$p < 0.05$, **$p < 0.01$, and ***$p < 0.001$.

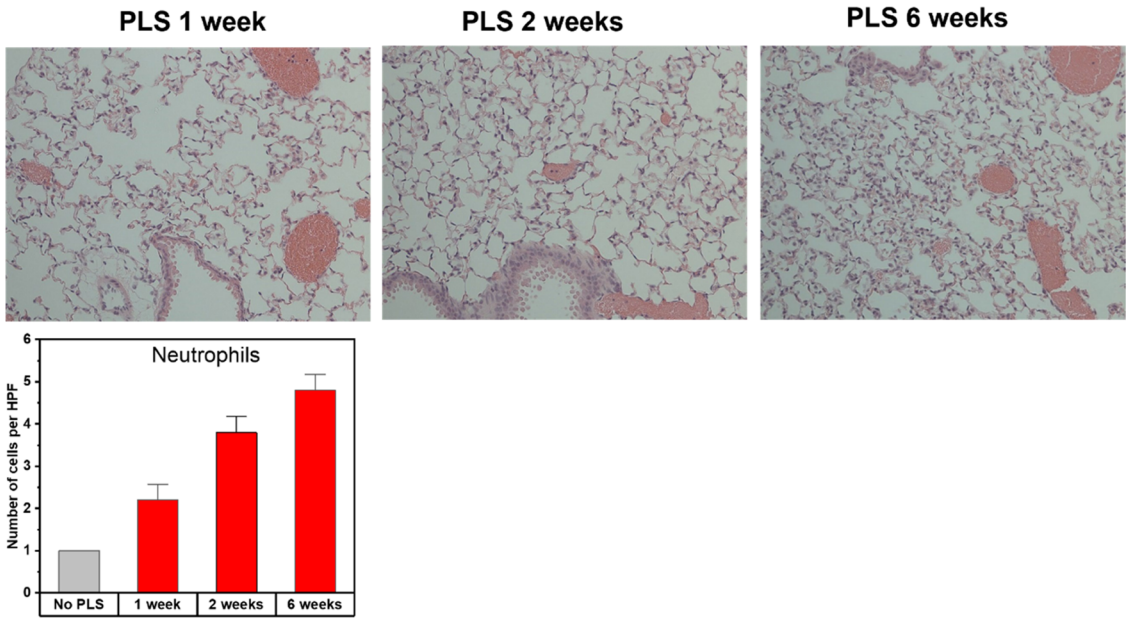

Figure 9. Histological analysis of long-term safety of PLS. Representative hematoxylin-and-eosin (H&E)-stained sections of lungs treated with PLS. To quantify neutrophils, five regions of H&E slides were analyzed under a high-magnification microscope and number of neutrophils were counted per high power field (HPF). WT C57BL/6 mice were treated with 90 μL of PLS (0.6 mg/mL in 0.9% saline) instilled into bilateral lungs using pharyngeal administration ($N = 3$).

https://doi.org/10.1021/acsbiomaterials.3c00061
ACS Biomater. Sci. Eng. 2023, 9, 2716−2730

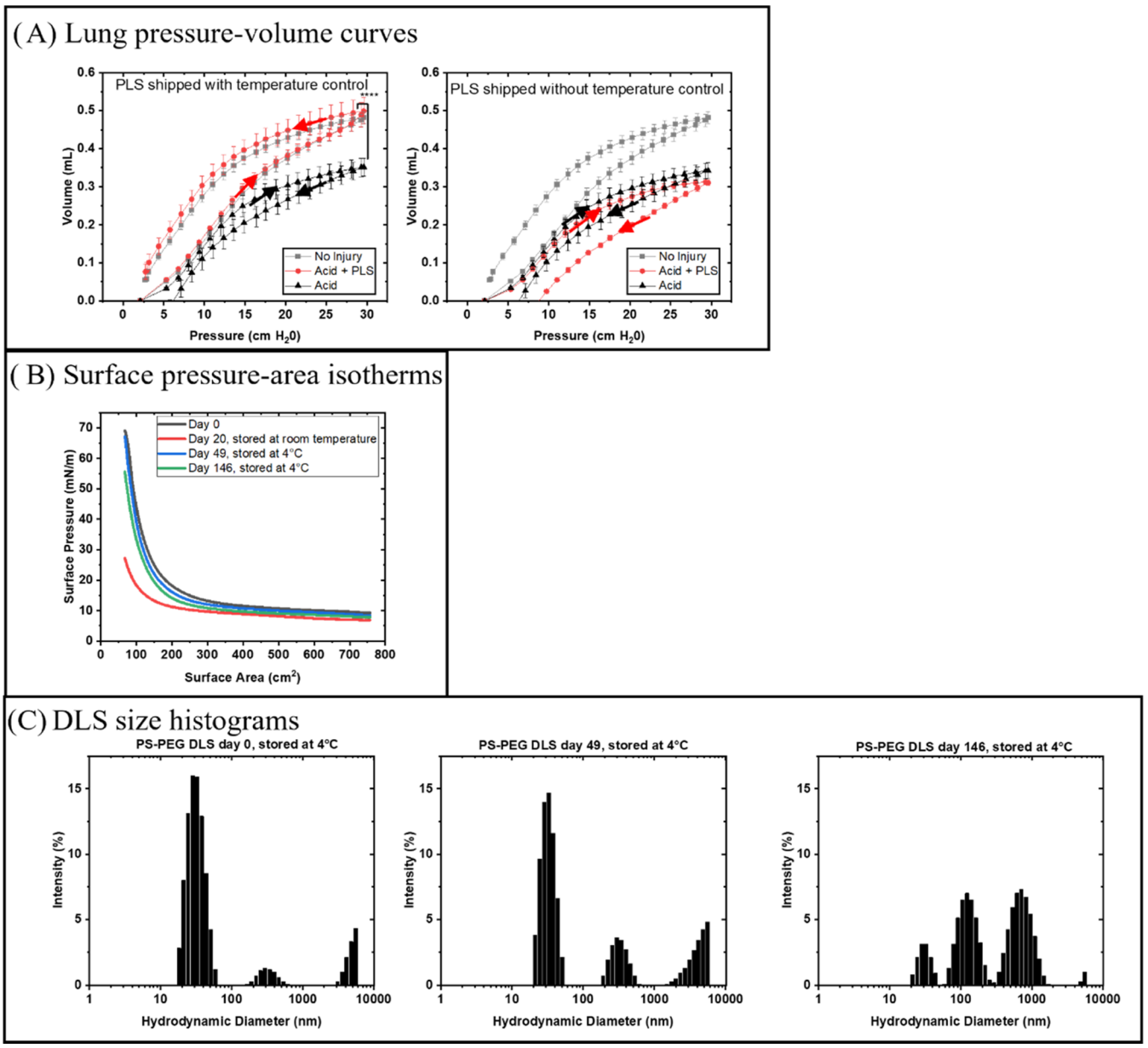

Figure 10. Effect of PLS storage conditions on efficacy and stability. Effect of storage conditions on (A) pressure−volume (PV) curves for acid-induced lung injury 29 h after acid insult, (B) surface pressure−area isotherms for water-spread PS-PEG micelles (5 mg/mL, 100 μL) on the water surface, and (C) DLS hydrodynamic size distribution.

significantly lower after PLS treatment for both time points, whereas the tumor necrosis factor (inflammatory cytokine produced by macrophages) was significantly lower only at 29 h after LPS-induced injury. Macrophage inhibitor protein-2 (MIP-2) and keratinocyte chemoattractant (KC), which are members of the platelet factor 4 cytokine superfamily, were significantly lower for the PLS group at 29 h after LPS injury. The inflammatory enzyme MPO was greatly increased after injury for both treatment and nontreatment groups, and there were no statistical differences between groups. The PLS treatment showed the ability to reduce both alveolar permeability and levels of multiple inflammatory markers following LPS injury.

Additionally, the expressions of hypoxic markers, HIF-1α and VEGF-A, were measured using real-time PCR on whole-lung tissue 29 h after LPS instillation. The results given in Figure 7C show that PLS treatment led to a significantly lower expression of both genes. Therefore, similar to the acid-injury case, the results suggest that PLS limited hypoxic conditions up to 29 h following LPS instillation.

To assess changes in active surfactant concentration and composition, a lipidomics analysis was done in the same manner as previously described for the acid-injury model. The results (Figure 8) show that the PLS treatment led to a significant increase in the absolute recovery of all six PC lipids at 29 h after LPS injury compared to the LPS-only group. At 53 h, the PLS treatment led to a significant increase in the recovery of DPPC, the most abundant PC lipid, as well as the less abundant lipids PMPC and PoOPC. Interestingly, LPS injury led to a significant enrichment in the relative DPPC amount; furthermore, PLS mitigated this effect at 29 h but not at 53 h after LPS injury. Additionally, the ratio of total amount of the six measured PC lipids to LysoPC 16:0 was significantly increased at 29 h post LPS injury for the PLS treatment group.

https://doi.org/10.1021/acsbiomaterials.3c00061
ACS Biomater. Sci. Eng. 2023, 9, 2716−2730

The PLS treatment was able to mitigate changes to the natural surfactant after LPS injury by mitigating the depletion of large surfactant aggregates and the enzymatic degradation of PC lipids.

3.4. Long-Term Safety and Stability of PLS Formulation. Given that the PLS particles are expected to reside within the lung on the order of several weeks,[12] the long-term safety of the formulation must be examined. The long-term safety of PLS was analyzed using histology of mice at 1, 2, and 6 weeks after receiving PLS instillation. The results (Figure 9) show mice receiving PLS displayed no indication of thickening/accumulation of eosinophilic material or granuloma for the 6-week period; however, there is a slight increase in the number of neutrophils compared to the control. The magnitude of neutrophils from PLS treatment alone is an order of magnitude lower than the amount induced by acid injury, indicating PLS particles cause a minor but nonnegligible immune response in mice.

Another important property of nanoparticle suspensions, like the PLS formulation, is their stability. Preventing dynamic changes in size characteristics is especially important in the case of PLS where the size affects the desired material properties.[17] As a demonstration of this point, a comparison of the efficacy, as measured by the lung PV curves at 29 h post acid-induced injury, for the PLS treatment under two different shipment conditions is shown in Figure 10A. One shipment condition was using FedEx standard shipping with no temperature control where the temperature is expected to have been room temperature or higher (20−25 °C); the sample remained for 5 days in these conditions, i.e., during the FedEx delivery from the location of formulation (Purdue University) to the location of experimentation (University of Michigan). The other sample was delivered by personal car in 1 day with temperature control (0−4 °C). The results in Figure 10A indicate that the shipping conditions significantly affected the efficacy of the PLS formulation. As previously explained, the PLS sample shipped carefully with temperature control produced a significant improvement in PV mechanics compared to the injury-only group. However, the PLS formulation shipped with no temperature control led to no significant improvements and worsened the lung mechanics compared to injury only. The differences in efficacy imply that the properties of PLS nanoparticle liquid suspension changed when exposed to elevated temperature for several days.

To investigate the changes in efficacy of the PLS formulation under different shipment conditions, the surface pressure−area isotherms of the PLS formulation over time in different storage conditions were measured. Figure 10B shows surface pressure−area isotherms for a solution stored at room temperature for 20 days and a sample stored at 4 °C for 164 days with isotherm data shown for day 49 and day 146. The samples stored at room temperature for 20 days showed a significant shift to lower areas, indicating a loss of surface-active material (likely due to the sedimentation of large aggregates). However, the sample stored at 4 °C showed only a slight shift to lower areas after 164 days, indicating that the original surface-mechanical properties were largely preserved.

To analyze if storing at 4 °C can stabilize against aggregation, DLS measurements were also taken over the 164-day period. Figure 10C shows DLS intensity(I)-weighted hydrodynamic diameter (D_h) size histograms for PS-PEG samples stored at 4 °C at Day 0, Day 49, and Day 164. The DLS histograms show little change in the first 40 days, with the highest intensity peak occurring around 30 nm. After 164 days, the highest intensities are shifted to populations around 100 and 1000 nm. Considering that DLS intensity scales as $I-D_h^6$ and volume (V) scales as $V-D_h^3$, the volume ratio of two populations is $V_1/V_2 = (I_1/I_2)\cdot(D_{h,2}/D_{h,1})^3$. Therefore, the population centered around 100 nm makes up around 6% by volume, and the population centered at 1000 nm makes up less than 0.01% by volume, indicating that there was a non-negligible amount of small micelle aggregates (containing a few tens of micelles), but the number of larger aggregates was suppressed.

4. DISCUSSION

Surfactant deactivation/denaturation is widely accepted as a contributing factor to the progression of lung injury following an insult, whether direct or indirect. Also, inadequate production of the lung surfactant caused by direct damage to type II alveolar epithelial cells contributes to lung injury. The initial lung injury, either by direct damage or by the resulting neutrophilic infiltration, results in damage to the endothelial and epithelial layer causing leakage of pulmonary edema into the alveolus. The surface-active proteins (including albumin and other serum proteins) contained within the edema then cause the deactivation of the lung surfactant.[22,34] The deactivation of the surfactant results in high alveolar surface tension that has been shown to increase the magnitude of edema flooding.[35] Additionally, the high surface tension causes the alveoli and small airways to be more susceptible to collapse during expiration.[36] As regions of the lung begin to collapse, it becomes highly heterogeneous, creating regions that experience elevated levels of strain. The increase in regional strain has been shown to trigger further inflammatory response and edema leading to a dangerous cycle of symptoms. Due to the contribution of surfactant deactivation to the progression of lung injury/inflammation, surfactant replacement therapy (SRT) provides a promising route for the mitigation of the severity of lung injury.

We have tested SRT in two models of lung injury (acid-induced and LPS-induced) using a novel PLS by administration at 5 h after the initial injury. Both injury models showed direct evidence of surfactant dysfunction as the total concentration of PC lipids in large aggregates was reduced over 10-fold at the peak of injury (29 h for acid and 53 h for LPS), similar to what has been shown in other models of lung injury.[26,37] By administering PLS in the second phase of neutrophil-mediated injury, before alveolar permeability had reached its peak, PLS treatment significantly affected the trajectory of the injury symptoms. The histology images shown in Figure 3 provide clear evidence that the administration of PLS reduced the extent of diffusive alveolar damage that is interpreted as a direct result of PLS restoring the low air−water surface-tension condition within the alveoli. This is consistent with the improved mechanical function of the lung at 29 h after acid-induced injury (Figure 5) as the PLS-treated lung shows improved lung compliance during inflation (less pressure is required to generate the same increase in volume) and recoils at a slower rate. The current results complement our previous finding that PLS is more effective than phospholipid-based surfactant replacement formulations at improving compliance immediately after PLS administration at 5 h after acid-induced injury.[8] The ability of PLS to maintain its surface-tension-lowering properties even in the presence of surface-active blood proteins allows it to stabilize the alveoli in

https://doi.org/10.1021/acsbiomaterials.3c00061
ACS Biomater. Sci. Eng. 2023, 9, 2716−2730

an inflammatory environment. Since surfactant deactivation has been linked to increased alveolar permeability,[38] the lower levels of albumin at all measured time points post PLS administration also provide evidence that PLS is effectively reducing the air−water surface tension within the alveoli.

PLS treatment also led to a reduction of inflammatory markers (IL-6 and IL-1β in acid injury, and IL-1β and MIP-2 in LPS injury), which suggests that surfactant dysfunction indeed contributed to the inflammatory response in these models. Therefore, although the lung injury models in the present study were completed without supraphysiologic amounts of mechanical stress (no mechanical ventilation was used), there is still a high probability that there were sufficiently high amounts of regional strain in order to induce mechanotransduction-induced inflammatory responses in the acutely injured lungs. Furthermore, we propose that the PLS treatment, by preventing alveolar collapse and improving lung homogeneity, was able to mitigate the levels of high regional strain and the subsequent inflammatory response. The anti-inflammatory effects of PLS treatment suggest that there is a mitigation of the mechanotransduction pathway of the inflammatory response during lung injury. PLS treatment also improved the quasi-static compliance of the lung that is a sensitive indicator of lung injury/inflammation. Mechanotransduction, the process by which mechanical forces induce a intracellular signal, has been shown to induce activation of pulmonary inflammation as well as extracellular matrix (ECM) and cytoskeleton remodeling when the lung is exposed to elevated levels of mechanical stress.[39] Lungs suffering from acute injury are susceptible to high levels of regional strain due to their heterogeneity as some portions of alveoli retain normal functioning while other portions are collapsed. Since the collapsed portions have limited air capacity, the inspired volume is preferentially directed toward noncollapsed regions such that abnormal alveolar volumetric strain can occur. A recent study using CT imaging demonstrated a strong correlation between regions of high volumetric strain and regions of elevated inflammatory response providing evidence that volumetric strain is a trigger for mechanotransduction-induced inflammation.[40] Also, an in vitro study showed that alveolar macrophages subjected to cyclic stretch leads to release of IL-1β, which has also shown to be released during lung injury.[41]

Although the injurious effects of high mechanical stress are commonly reported in the context of ventilation-induced lung injury (VILI),[42] spontaneous breathing in injured lungs has also been shown to generate regions of high strain similar to that which can occur during nonprotective mechanical ventilation.[43] The development of lung injuries from high respiratory drive during respiratory disease is known as patient self-inflicted lung injury (P-SILI).[44] P-SILI has been suggested to occur in spontaneously breathing COVID-19 patients who showed significantly higher levels of regional strain than healthy control subjects.[45] Evidence for surfactant dysfunction alone being able to generate an inflammatory response has been shown by studying spontaneously breathing mice with conditional expression of surface protein B (SP-B)[46] When mice were made SP-B-deficient (without any other imposed injury), the levels of protein in BAL, IL-6, IL-1β, and MIP-2 were significantly increased, which corresponded with higher values of minimum surface tension for the extracted surfactant.[46] Additionally, the inflammatory response was found to be reversible by reversal of SP-B expression.[46] The potential of SRT to reduce the inflammatory response when surfactant dysfunction occurs was demonstrated in a bleomycin-induced injury model where SRT led to a reduction of IL-6, IL-1β, and the protein in BAL.[47]

Another possible contribution to the anti-inflammatory activity of PLS is the inherent protective properties of PEG, the hydrophilic component of PLS, which has been demonstrated only in a few select cases. For example, intravenous treatment with a high-molecular-weight (35 kDa) PEG dose (10 mg/kg body weight) following acute necrotizing pancreatitis has been shown to lower lung inflammatory response in rats.[48] Additionally, a 8% PEG 15−20 kDa solution has been shown in vitro to enhance pulmonary vascular endothelial integrity and reduce permeability.[49] Although these studies provide evidence that PEG can produce anti-inflammatory effects (particularly through protection of the endothelial membrane), it is not clear whether the dosage of PEG (1.2 mg/kg body weight) and molecular weight (5 kDa) used in PLS treatment can produce the anti-inflammatory effects seen in previous studies. Additionally, given that the PLS forms an insoluble monolayer, the PS-PEG nanoparticles are expected to be located primarily at the alveoli air−water interface and not at significant concentrations near the endothelial layer.

A crucial finding of this study is that PLS affects the composition of lung surfactants. PLS treatment mitigates the loss of DPPC, the most potent component of the lung surfactant, from large surfactant aggregates in both acid-injured and LPS-injured lungs at the point when injury was most severe (29 h for acid injury and 53 h for LPS injury). However, the PLS did not serve to promote the restoration to normal natural surfactant levels during the time frame of this study as both the PLS-treated and nontreated groups showed depleted levels of natural surfactant at 53 h post injury. Therefore, longer time points will be needed to draw more definitive conclusions on the impact of PLS on the restoration of natural lung surfactant following injury. Lastly, PLS reduces the level of LysoPC, an enzymatic degradation product of PC produced during lung injury. It remains to be investigated whether PLS is directly involved in producing this effect or is indirectly involved through its impact in reducing acute inflammation.

5. CONCLUSIONS

Using a novel PLS as a treatment for ARDS has been demonstrated using two different models of lung injury in mice. By applying the treatment in the early onset of acute injury symptoms, the PLS was able to mitigate the progression of lung injury as shown by histopathology, lung compliance, levels of albumin in BAL, levels of hypoxia markers, levels of proinflammatory cytokines in BAL and lung tissue, total amounts of PC lipids, and relative amounts of LysoPC recovered in large surfactant aggregates. For the PLS to be successfully translated into a clinical therapy for patients suffering from ARDS, further considerations must be given to optimal dose, formulation of lung delivery, and long-term storage.

■ ASSOCIATED CONTENT

Supporting Information

The Supporting Information is available free of charge at https://pubs.acs.org/doi/10.1021/acsbiomaterials.3c00061.

https://doi.org/10.1021/acsbiomaterials.3c00061
ACS Biomater. Sci. Eng. 2023, 9, 2716−2730

DLS hydrodynamic size distribution of PS-PEG micelles in water, samples were measured at a concentration of 1 mg/mL and were filtered using 0.45 μm syringe filters (PDF)

AUTHOR INFORMATION

Corresponding Authors

Krishnan Raghavendran − *Department of Surgery, University of Michigan Medical School, Ann Arbor, Michigan 48109, United States*; Phone: +1-734-936-5738; Email: kraghave@med.umich.edu

You-Yeon Won − *Davidson School of Chemical Engineering, Purdue University, West Lafayette, Indiana 47907, United States; Purdue University Center for Cancer Research, Purdue University, West Lafayette, Indiana 47907, United States;* orcid.org/0000-0002-8347-6375; Phone: +1-765-494-4077; Email: yywon@purdue.edu

Authors

Daniel J. Fesenmeier − *Davidson School of Chemical Engineering, Purdue University, West Lafayette, Indiana 47907, United States*

Madathilparambil V. Suresh − *Department of Surgery, University of Michigan Medical School, Ann Arbor, Michigan 48109, United States*

Seyoung Kim − *Davidson School of Chemical Engineering, Purdue University, West Lafayette, Indiana 47907, United States*

Sungwan Park − *Davidson School of Chemical Engineering, Purdue University, West Lafayette, Indiana 47907, United States*

Complete contact information is available at: https://pubs.acs.org/10.1021/acsbiomaterials.3c00061

Author Contributions

‖D.J.F. and M.V.S. contributed equally to this work.

Notes

The authors declare the following competing financial interest(s): YYW has an ownership interest in a startup company, Spirrow Therapeutics, which is currently attempting to commercialize the technology disclosed in the present manuscript.

ACKNOWLEDGMENTS

The authors are grateful for funding from NSF (IIP-2036125, CBET-2211843) and Spirrow Therapeutics. The authors also acknowledge support from the Purdue University Center for Cancer Research (PCCR) via an NIH NCI Grant (P30 CA023168), which supports the campus-wide NMR-shared resources that were utilized in this work as well as Purdue University's Metabolite Profiling Facility (MPF), especially Dr. Christina R. Ferriera, in the acquisition and analysis of mass spectrometry data presented in Figures 6 and 8. The authors are grateful to Prof. Bennett D. Elzey and Sandra E. Torregrosa-Allen at the Biological Evaluation Shared Resource (BE-SR) facility of the PCCR for their assistance with collecting data presented in Figure 2. The authors also acknowledge that the graphical abstract was created with BioRender.com.

REFERENCES

(1) Polin, R. A.; Carlo, W. A.; Papile, L. A.; Polin, R. A.; Carlo, W.; Tan, R.; Kumar, P.; Benitz, W.; Eichenwald, E.; Cummings, J.; Baley, J.; et al. Surfactant Replacement Therapy for Preterm and Term Neonates With Respiratory Distress. *Pediatrics* **2014**, *133*, 156−163.

(2) Kesecioglu, J.; Beale, R.; Stewart, T. E.; Findlay, G. P.; Rouby, J. J.; Holzapfel, L.; Bruins, P.; Steenken, E. J.; Jeppesen, O. K.; Lachmann, B. Exogenous natural surfactant for treatment of acute lung injury and the acute respiratory distress syndrome. *Am. J. Respir. Crit. Care Med.* **2009**, *180*, 989−994.

(3) Spadaro, S.; Park, M.; Turrini, C.; Tunstall, T.; Thwaites, R.; Mauri, T.; Ragazzi, R.; Ruggeri, P.; Hansel, T. T.; Caramori, G.; Volta, C. A. Biomarkers for Acute Respiratory Distress syndrome and prospects for personalised medicine. *J. Inflammation* **2019**, *16*, No. 1.

(4) Seeger, W.; Grube, C.; Günther, A.; Schmidt, R. Surfactant inhibition by plasma proteins: differential sensitivity of various surfactant preparations. *Eur. Respir. J.* **1993**, *6*, 971−977. Holm, B. A.; Matalon, S. Role of pulmonary surfactant in the development and treatment of adult respiratory distress syndrome. *Anesth. Analg.* **1989**, *69*, 805−818. Machado-Aranda, D.; Wang, Z.; Yu, B.; Suresh, M. V.; Notter, R. H.; Raghavendran, K. Increased phospholipase A2 and lyso-phosphatidylcholine levels are associated with surfactant dysfunction in lung contusion injury in mice. *Surgery* **2013**, *153*, 25−35.

(5) Kim, H. C.; Won, Y.-Y. Clinical, technological, and economic issues associated with developing new lung surfactant therapeutics. *Biotechnol. Adv.* **2018**, *36*, 1185−1193.

(6) Bellani, G.; Laffey, J. G.; Pham, T.; Fan, E.; Brochard, L.; Esteban, A.; Gattinoni, L.; van Haren, F.; Larsson, A.; McAuley, D. F.; et al. Epidemiology, Patterns of Care, and Mortality for Patients With Acute Respiratory Distress Syndrome in Intensive Care Units in 50 Countries. *JAMA* **2016**, *315*, 788−800.

(7) Zhang, H.; Wang, Y. E.; Fan, Q.; Zuo, Y. Y. On the Low Surface Tension of Lung Surfactant. *Langmuir* **2011**, *27*, 8351−8358.

(8) Kim, H. C.; Suresh, M. V.; Singh, V. V.; Arick, D. Q.; Machado-Aranda, D. A.; Raghavendran, K.; Won, Y.-Y. Polymer Lung Surfactants. *ACS Appl. Bio Mater.* **2018**, *1*, 581−592.

(9) Suresh, M. V.; Dolgachev, V. A.; Zhang, B.; Balijepalli, S.; Swamy, S.; Mooliyil, J.; Kralovich, G.; Thomas, B.; Machado-Aranda, D.; Karmakar, M.; et al. TLR3 absence confers increased survival with improved macrophage activity against pneumonia. *JCI Insight* **2019**, *4*, No. e131195.

(10) Suresh, M. V.; Yalamanchili, G.; Rao, T.; Aktay, S.; Kralovich, A.; Shah, Y.; Raghavendran, K. Hypoxia-Inducible Factor (HIF)-1α induced regulation of lung injury in pulmonary aspiration is mediated through NF-kB. *FASEB BioAdv.* **2021**, *4*, 309−328.

(11) Suresh, M. V.; Balijepalli, S.; Zhang, B.; Singh, V. V.; Swamy, S.; Panicker, S.; Dolgachev, V. A.; Subramanian, C.; Ramakrishnan, S. K.; Thomas, B.; et al. Hypoxia-Inducible Factor (HIF)-1α Promotes Inflammation and Injury Following Aspiration-Induced Lung Injury in Mice. *Shock* **2019**, *52*, 612−621.

(12) Kim, S.; Fesenmeier, D. J.; Park, S.; Torregrosa-Allen, S. E.; Elzey, B. D.; Won, Y.-Y. Pulmonary Pharmacokinetics of Polymer Lung Surfactants Following Pharyngeal Administration in Mice. *Biomacromolecules* **2022**, *23*, 2471−2484.

(13) Suresh, M. V.; Yu, B.; Machado-Aranda, D.; Bender, M. D.; Ochoa-Frongia, L.; Helinski, J. D.; Davidson, B. A.; Knight, P. R.; Hogaboam, C. M.; Moore, B. B.; Raghavendran, K. Role of macrophage chemoattractant protein-1 in acute inflammation after lung contusion. *Am. J. Respir. Cell Mol. Biol.* **2012**, *46*, 797−806.

(14) Bligh, E. G.; Dyer, W. J. A rapid method of total lipid extraction and purification. *Can. J. Biochem. Physiol.* **1959**, *37*, 911−917.

(15) de Lima, C. B.; Ferreira, C. R.; Milazzotto, M. P.; Sobreira, T. J. P.; Vireque, A. A.; Cooks, R. G. Comprehensive lipid profiling of early stage oocytes and embryos by MRM profiling. *J. Mass Spectrom.* **2018**, *53*, 1247−1252.

(16) Neises, B.; Steglich, W. Simple Method for the Esterification of Carboxylic Acids. *Angew. Chem., Int. Ed.* **1978**, *17*, 522−524.

(17) Fesenmeier, D. J.; Park, S.; Kim, S.; Won, Y.-Y. Surface mechanical behavior of water-spread poly(styrene)−poly(ethylene glycol) (PS−PEG) micelles at the air−water interface: Effect of micelle size and polymer end/linking group chemistry. *J. Colloid Interface Sci.* **2022**, *617*, 764−777.
(18) Filoche, M.; Tai, C. F.; Grotberg, J. B. Three-dimensional model of surfactant replacement therapy. *Proc. Natl. Acad. Sci. U.S.A.* **2015**, *112*, 9287−9292.
(19) Zhao, J. N.; Liu, Y.; Li, H. C. Aspiration-related acute respiratory distress syndrome in acute stroke patient. *PLoS One* **2015**, *10*, No. e0118682.
(20) Matute-Bello, G.; Frevert, C. W.; Martin, T. R. Animal models of acute lung injury. *Am. J. Physiol.-Lung Cell. Mol. Physiol.* **2008**, *295*, L379−L399.
(21) Raghavendran, K.; Davidson, B. A.; Mullan, B. A.; Hutson, A. D.; Russo, T. A.; Manderscheid, P. A.; Woytash, J. A.; Holm, B. A.; Notter, R. H.; Knight, P. R. Acid and particulate-induced aspiration lung injury in mice: importance of MCP-1. *Am. J. Physiol.-Lung Cell. Mol. Physiol.* **2005**, *289*, L134−L143.
(22) Taeusch, H. W.; de la Serna, J. B.; Perez-Gil, J.; Alonso, C.; Zasadzinski, J. A. Inactivation of pulmonary surfactant due to serum-inhibited adsorption and reversal by hydrophilic polymers: experimental. *Biophys. J.* **2005**, *89*, 1769−1779.
(23) Rincon, M.; Irvin, C. G. Role of IL-6 in Asthma and Other Inflammatory Pulmonary Diseases. *Int. J. Biol. Sci.* **2012**, *8*, 1281−1290.
(24) Schmitz, N.; Kurrer, M.; Bachmann Martin, F.; Kopf, M. Interleukin-1 Is Responsible for Acute Lung Immunopathology but Increases Survival of Respiratory Influenza Virus Infection. *J. Virol.* **2005**, *79*, 6441−6448.
(25) Haegens, A.; Vernooy, J. H.; Heeringa, P.; Mossman, B. T.; Wouters, E. F. Myeloperoxidase modulates lung epithelial responses to pro-inflammatory agents. *Eur. Respir. J.* **2008**, *31*, 252−260.
(26) Raghavendran, K.; Davidson, B. A.; Knight, P. R.; Wang, Z.; Helinski, J.; Chess, P. R.; Notter, R. H. Surfactant Dysfunction in Lung Contusion with and Without Superimposed Gastric Aspiration in a Rat Model. *Shock* **2008**, *30*, 508−517.
(27) Semenza, G. L.; Wang, G. L. A nuclear factor induced by hypoxia via de novo protein synthesis binds to the human erythropoietin gene enhancer at a site required for transcriptional activation. *Mol. Cell. Biol.* **1992**, *12*, 5447−5454.
(28) Bermel, M. S.; McBride, J. T.; Notter, R. H. Lavaged excised rat lungs as a model of surfactant deficiency. *Lung* **1984**, *162*, 99−113. Johnson, J. W. C.; Permutt, S.; Sipple, J. H.; Salem, E. S. Effect of intra-alveolar fluid on pulmonary surface tension properties. *J. Appl. Physiol.* **1964**, *19*, 769−777.
(29) Gross, N. J.; Narine, K. R. Surfactant subtypes in mice: characterization and quantitation. *J. Appl. Physiol.* **1989**, *66*, 342−349.
(30) Notter, R. H.*Lung surfactants: Basic Science and Clinical Applications*; CRC Press, 2000.
(31) Hurley, B. P.; McCormick, B. A. Multiple roles of phospholipase A2 during lung infection and inflammation. *Infect. Immun.* **2008**, *76*, 2259−2272. Arbibe, L.; Koumanov, K.; Vial, D.; Rougeot, C.; Faure, G.; Havet, N.; Longacre, S.; Vargaftig, B. B.; Béréziat, G.; Voelker, D. R.; et al. Generation of lyso-phospholipids from surfactant in acute lung injury is mediated by type-II phospholipase A2 and inhibited by a direct surfactant protein A-phospholipase A2 protein interaction. *J. Clin. Invest.* **1998**, *102*, 1152−1160.
(32) Barman, S.; Davidson, M. L.; Walker, L. M.; Anna, S. L.; Zasadzinski, J. A. Inflammation product effects on dilatational mechanics can trigger the Laplace instability and acute respiratory distress syndrome. *Soft Matter* **2020**, *16*, 6890−6901.
(33) Chen, H.; Bai, C.; Wang, X. The value of the lipopolysaccharide-induced acute lung injury model in respiratory medicine. *Expert Rev. Respir. Med.* **2010**, *4*, 773−783.
(34) Zasadzinski, J. A.; Stenger, P. C.; Shieh, I.; Dhar, P. Overcoming rapid inactivation of lung surfactant: Analogies between competitive adsorption and colloid stability. *Biochim. Biophys. Acta, Biomembr.* **2010**, *1798*, 801−828.
(35) Nieman, G. F.; Bredenberg, C. E. High surface tension pulmonary edema induced by detergent aerosol. *J. Appl. Physiol.* **1985**, *58*, 129−136. Bredenberg, C. E.; Paskanik, A. M.; Nieman, G. F. High surface tension pulmonary edema. *J. Surg. Res.* **1983**, *34*, 515−523.
(36) Carney, D.; DiRocco, J.; Nieman, G. Dynamic alveolar mechanics and ventilator-induced lung injury. *Crit. Care Med.* **2005**, *33*, S122−S128. DiRocco, J. D.; Pavone, L. A.; Carney, D. E.; Lutz, C. J.; Gatto, L. A.; Landas, S. K.; Nieman, G. F. Dynamic alveolar mechanics in four models of lung injury. *Intensive Care Med.* **2006**, *32*, 140−148.
(37) Hall, S. B.; Hyde, R. W.; Notter, R. H. Changes in subphase aggregates in rabbits injured by free fatty acid. *Am. J. Respir. Crit. Care Med.* **1994**, *149*, 1099−1106. Davidson, B. A.; Knight, P. R.; Wang, Z.; Chess, P. R.; Holm, B. A.; Russo, T. A.; Hutson, A.; Notter, R. H. Surfactant alterations in acute inflammatory lung injury from aspiration of acid and gastric particulates. *Am. J. Physiol.-Lung Cell. Mol. Physiol.* **2005**, *288*, L699−708.
(38) Díaz, F.; Erranz, B.; Donoso, A.; Carvajal, C.; Salomón, T.; Torres, M.; Cruces, P. Surfactant deactivation in a pediatric model induces hypovolemia and fluid shift to the extravascular lung compartment. *Pediatr. Anesth.* **2013**, *23*, 250−257.
(39) Lin, C.; Zheng, X.; Lin, S.; Zhang, Y.; Wu, J.; Li, Y. Mechanotransduction Regulates the Interplays Between Alveolar Epithelial and Vascular Endothelial Cells in Lung. *Front. Physiol.* **2022**, *13*, No. 246.
(40) Retamal, J.; Hurtado, D.; Villarroel, N.; Bruhn, A.; Bugedo, G.; Amato, M. B. P.; Costa, E. L. V.; Hedenstierna, G.; Larsson, A.; Borges, J. B. Does Regional Lung Strain Correlate With Regional Inflammation in Acute Respiratory Distress Syndrome During Nonprotective Ventilation? An Experimental Porcine Study*. *Crit. Care Med.* **2018**, *46*, e591−e599.
(41) Wu, J.; Yan, Z.; Schwartz, D. E.; Yu, J.; Malik, A. B.; Hu, G. Activation of NLRP3 Inflammasome in Alveolar Macrophages Contributes to Mechanical Stretch-Induced Lung Inflammation and Injury. *J. Immunol.* **2013**, *190*, 3590−3599.
(42) Slutsky, A. S.; Ranieri, V. M. Ventilator-Induced Lung Injury. *N. Engl. J. Med.* **2013**, *369*, 2126−2136.
(43) Hurtado, D. E.; Erranz, B.; Lillo, F.; Sarabia-Vallejos, M.; Iturrieta, P.; Morales, F.; Blaha, K.; Medina, T.; Diaz, F.; Cruces, P. Progression of regional lung strain and heterogeneity in lung injury: assessing the evolution under spontaneous breathing and mechanical ventilation. *Ann. Intensive Care* **2020**, *10*, No. 107.
(44) Brochard, L.; Slutsky, A.; Pesenti, A. Mechanical Ventilation to Minimize Progression of Lung Injury in Acute Respiratory Failure. *Am. J. Respir. Crit. Care Med.* **2017**, *195*, 438−442.
(45) Pulletz, S.; Krukewitt, L.; Gonzales-Rios, P.; Teschendorf, P.; Kremeier, P.; Waldmann, A.; Zitzmann, A.; Müller-Graf, F.; Acosta, C.; Tusman, G.; et al. Dynamic relative regional strain visualized by electrical impedance tomography in patients suffering from COVID-19. *J. Clin. Monit. Comput.* **2022**, *36*, 975−985.
(46) Ikegami, M.; Whitsett, J. A.; Martis, P. C.; Weaver, T. E. Reversibility of lung inflammation caused by SP-B deficiency. *Am. J. Physiol.-Lung Cell. Mol. Physiol.* **2005**, *289*, L962−L970.
(47) Steffen, L.; Ruppert, C.; Hoymann, H.-G.; Funke, M.; Ebener, S.; Kloth, C.; Mühlfeld, C.; Ochs, M.; Knudsen, L.; Lopez-Rodriguez, E. Surfactant replacement therapy reduces acute lung injury and collapse induration-related lung remodeling in the bleomycin model. *Am. J. Physiol.-Lung Cell. Mol. Physiol.* **2017**, *313*, L313−L327.
(48) Ferrero-Andrés, A.; Panisello-Roselló, A.; Serafín, A.; Roselló-Catafau, J.; Folch-Puy, E. Polyethylene glycol 35 (PEG35) protects against inflammation in experimental acute necrotizing pancreatitis and associated lung injury. *Int. J. Mol. Sci.* **2020**, *21*, No. 917.
(49) Chiang, E. T.; Camp, S. M.; Dudek, S. M.; Brown, M. E.; Usatyuk, P. V.; Zaborina, O.; Alverdy, J. C.; Garcia, J. G. N. Protective effects of high-molecular weight Polyethylene Glycol (PEG) in human lung endothelial cell barrier regulation: Role of actin cytoskeletal rearrangement. *Microvasc. Res.* **2009**, *77*, 174−186.

https://doi.org/10.1021/acsbiomaterials.3c00061
ACS Biomater. Sci. Eng. 2023, 9, 2716−2730